

TWO-PHASE BEHAVIORS IN METAL FOAM FLOW FIELD WITH INHOMOGENEOUS PORE DISTRIBUTION

Zhiming Bao, Kui Jiao*

State Key Laboratory of Engines, Tianjin University, 135 Yaguan Rd, Tianjin, China, 300350

*Corresponding author: kjiao@tju.edu.cn; tel: +86-22-27404460; fax: +86-22-27383362

ABSTRACT

Recently, metal foam (MF) flow field has exhibited its superiority on mass transfer and potentials on promoting the power density of PEM fuel cells. In this study, the geometry of MF is reconstructed through three-dimensional X-ray computational tomography. The single- and two-phase flow simulations are then carried out. It is found that the pores in MF are relatively inhomogeneous, which has rarely been considered in previous numerical studies. Moreover, the convective flow, water retention and water split up are the unique mass transfer characteristics observed. In addition, the contact angle of MF ligaments shows a dramatic influence on the water management.

Keywords: PEM fuel cell; Metal foam flow field; VOF model; Mass transfer

1. INTRODUCTION

In recent years, proton exchange membrane (PEM) fuel cell has gained much attention for automotive applications due to its high efficiency, low emission, long range and system robustness [1]. However, for a widespread commercialization, the power density of PEM fuel cells still needs improvement, for which a main issue is mass transfer [2]. With the increment of performance, the gas supply and water producing rate are both raised. How to control the two-phase flow in the flow field is becoming a crucial technical problem.

An effective way for the improvement of mass transfer is to optimize flow field/channel. Many efforts have been put on the conventional flow-channel optimization, but its inherent drawbacks can hardly be avoided [3]. Thus, new types of flow fields such as porous material flow field and three-dimensional (3-D) baffled flow field are proposed [4]. In this study, the two-phase flow characteristics of a metal foam (MF) flow field is studied by a volume of fluid (VOF) method. The real

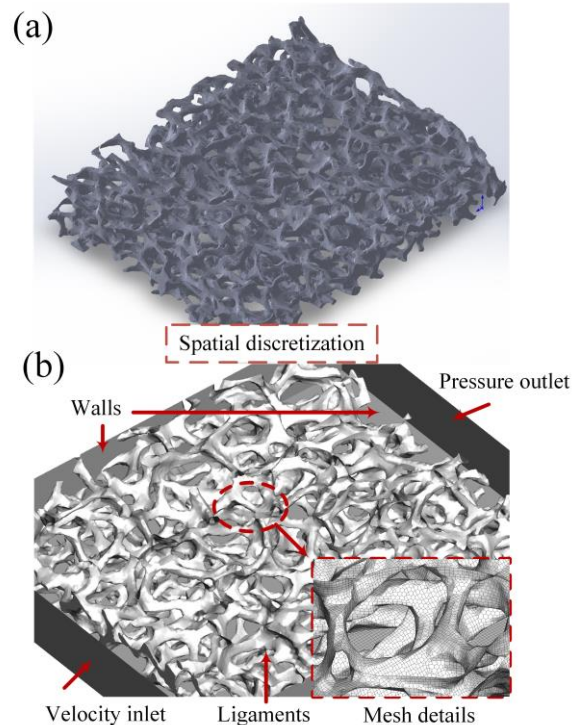


Fig 1 Reconstruction of MF flow field with real structure: (a) MF sample geometric profile, (b) MF flow field model.

structure of MF is reconstructed based on 3-D X-ray computational tomography (CT). The liquid behaviors and several physical parameters are then analyzed.

2. MODEL DEVELOPMENT

2.1 Reconstruction of MF flow field

Most of the reconstruction methods assume that the MF is composed of regular polyhedrons [5]. Though these methods have been verified effective on the study of two-phase flow, the non-homogeneous pore distribution was not considered. In this study, the MF sample geometry is captured by 3-D CT and a geometric file is gained after postprocess, as shown in Fig 1a. Then the flow field is spatially discretized with mesh size of 10

μm . The mesh details and boundary conditions of the model are shown in Fig. 1b.

It is notable that for a real PEM fuel cell, the water producing rate is too small for the water droplet to grow up [6]. Thus, the numerical study is carried out in two process: water accumulation process and air blowing processes. In the first process, water is injected from a $50 \times 50 \mu\text{m}^2$ pore on the lower surface in the first 5 ms. Then the droplet stays for the other 5 ms to balance its surface tension. In the second process, the air is blown in from gas inlet at a fixed velocity, and the analyses are mainly performed in this process.

The MF sample has a porosity of 0.81 and average pore diameter of 0.337 mm. The total size of flow field is $x \times y \times z = 3 \times 0.5 \times 3.6 \text{ mm}^3$, including MF flow field and two (inlet and outlet) sections. The contact angle of side walls, upper surface and lower surface are 90° , 90° and 130° , respectively. The inlet velocity v_i , droplet size R_d and contact angle θ_c range from $8 \sim 15 \text{ m s}^{-1}$, $80 \sim 160 \mu\text{m}$ and $120 \sim 150^\circ$, respectively.

2.2 Numerical method

A modified VOF method is used to study the incompressible two-phase laminar flow in the MF flow field model [6]. The phase fraction α is defined to track the phase interface:

$$\alpha = \begin{cases} 0, & \text{the cell is full of air} \\ 1, & \text{the cell is full of water} \\ (0, 1), & \text{the cell is at interface} \end{cases} \quad (1)$$

The mass, phase, momentum conservation equation, phase density and viscosity are all re-expressed based on α . For detailed explanation, readers can refer to [6].

The spatial discretization and two-phase flow simulation are both carried out on the open source software Open FOAM. About 5 million meshes were generated. Grid independence has been conducted with a doubled-grid-number model, showing a difference of gas velocity less than 5%. A scheme combining semi-implicit method for pressure linked equation (SIMPLE) with pressure-implicit with splitting of operators (PISO) is used to solve all the governing equations.

3. RESULT & DISCUSSION

3.1 Analysis of single-phase flow pattern

Fig 2a shows the velocity distribution in $y=0.25 \text{ mm}$ plane. It is obvious that the velocity is distributed non-uniformly because of the variation of pore diameter and porosity of the MF sample. It can be observed that where the local velocity is relatively larger (black dotted circles), the ligament (white part) is scarcely found, indicating a

better permeability with higher local porosity and pore diameter. The distribution of velocity may also cause non-uniformity on water behaviors because its effect on air drag force [7]. Then in Fig 2b, the vertical velocity distribution is exhibited, induced by the ligaments of MF which hinder the air flow and guide it transported in x-y plane. This characteristic makes the flow in MF flow field

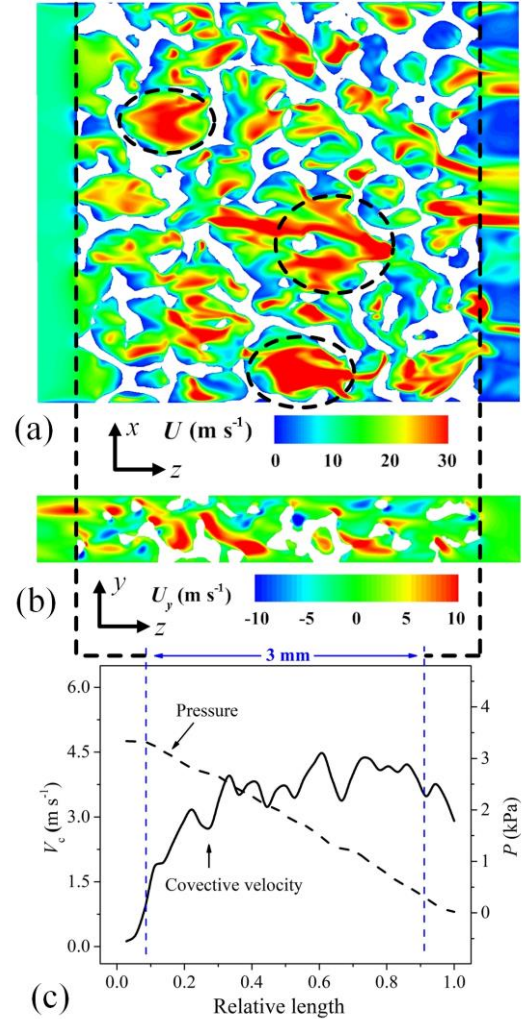


Fig 2 Single-phase flow pattern of MF flow field: (a) velocity distribution in x-z plane, (b) vertical velocity distribution in y-z plane, (c) vertical velocity and pressure distribution along z-axis.

more convective than that in conventional channel-rib structure, and the gas reactant transport mode varies from diffusion to convection-diffusion, largely enhancing the mass transfer efficiency [3]. The convective flow may also contribute to the water removal from GDL surface and avoid water blockage on GDL surface. To quantify the vertical velocity and permeability of MF flow field, the distribution of volume average convective velocity and pressure is plotted in Fig 2c, where the convective velocity is defined as:

$$V_c = \int |U_y| \cdot dV / V_b \quad (2)$$

where U_y is the absolute value of y-component of velocity, V_b the volume of the considered area. It is observed that the air flow becomes more convective in the whole flow field. Then the permeability of the MF flow field can be calculated according to pressure distribution and Darcy's Law [4]:

$$K = \frac{\mu L U_s}{\Delta P} \quad (3)$$

where μ is the viscosity of air, L the length of flow field, U_s the superficial velocity, ΔP the pressure difference. K of the flow field is calculated as $1.74 \times 10^{-10} \text{ m}^2$, a value much lower than conventional channels [3].

3.2 Analysis of two-phase behaviors

In this section, the two-phase characteristics in MF flow field are analyzed based on liquid behaviors and several physical parameters. The liquid droplet behaviors are visualized by the iso-surface of $\alpha_{\text{alpha}} = 0.5$ and the physical parameters include water saturation, water retention ratio and water coverage ratio.

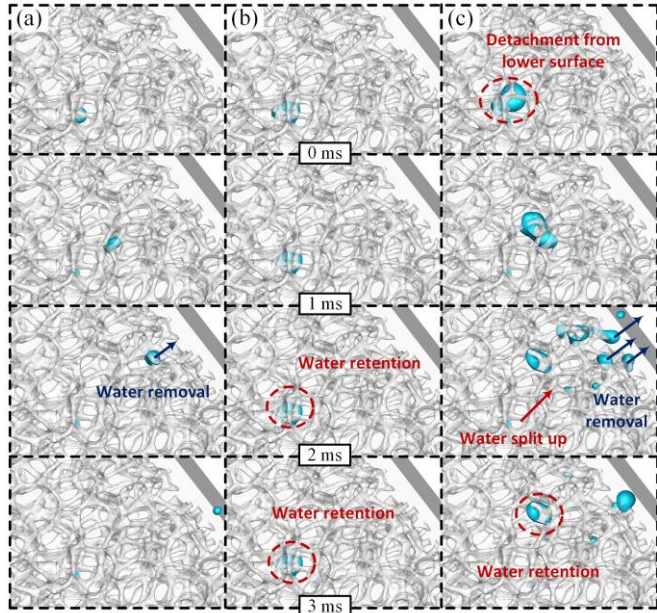


Fig 3 Liquid behaviors of droplets with size of (a) 80 μm , (b) 120 μm , (c) 160 μm .

The liquid behaviors of different droplets with inlet velocity of 10 m s^{-1} are shown in Fig 3. It is observed that for the smallest droplet (Fig 3a), all of the liquid remains in a whole volume and is finally removed from the flow field. Then, the middle size droplet (Fig 3b) is stagnant at the initial position. And the biggest droplet (Fig 3c) is split up under the air drag force and partly removed from the flow field. These phenomena verify the water retention characteristic of MF flow field, observed in previous studies [6, 8]. It is obvious that under the fixed inlet velocity and given MF flow field configuration, a droplet with radius smaller than a specific size, e.g., 80 μm in this

study, can be expelled from the flow field smoothly. But when the droplet accumulates to a certain volume, it will be retained in the pores of flow field because the air force on droplet cannot overcome the surface tension caused by the ligaments of MF [6, 7]. If the droplet continues to grow, it will be split up due to the cutting effect of ligament structures. Then the small droplets will be expelled from flow field while the others still stagnant in flow field.

To directly reflect the water retention characteristic of MF flow field, the water saturation is defined as:

$$s = \int \alpha dV / V_F \quad (4)$$

where V_F is the volume of whole MF flow field. The time variations of s are plotted in Fig 4. It is observed that for the droplets with same size, the water expelling rate and volume increase with inlet velocity. At $v_i = 15 \text{ m s}^{-1}$, the droplets with different sizes are totally expelled, while only a part of the biggest droplet is removed at $v_i = 8 \text{ m s}^{-1}$. Especially, for $R_d = 80, 120 \mu\text{m}$, the water is totally expelled once it is removed from initial position, but liquid still remains for droplet of $R_d = 160 \mu\text{m}$. The biggest droplet is firstly removed the from initial position due to the larger air drag force and then split up, and the relatively small droplets are expelled from the flow field, while the left part is retained in the pores near upper surface.

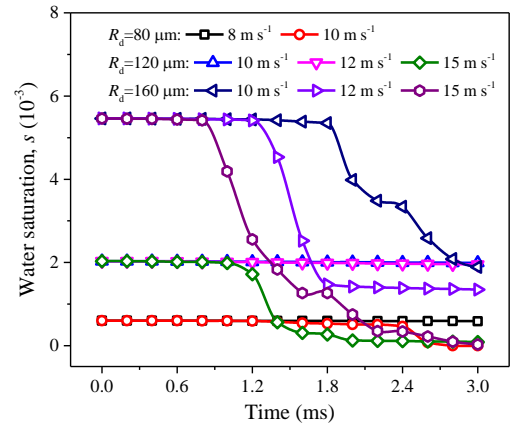


Fig 4 Time variations of water saturation s of cases with different inlet velocities and droplet sizes.

Then, the water retention and coverage ratio are also defined to compare the liquid behaviors of different cases, defined as:

$$\varepsilon_r = \int \alpha \cdot dV / V_d \quad (5)$$

$$\varepsilon_c = \int \alpha \cdot dS / S_F \quad (6)$$

where V_d is the initial droplet volume, S_F the total area of interface between GDL and flow field (GDL/FF interface), S the covered area by water. The final ε_r and ε_c of different droplet sizes and inlet velocities are plotted in Fig 5. The final water retention ratio decreases with inlet velocity but doesn't show a clear relation with

droplet size because of the liquid behavior characteristic mentioned above. The liquid coverage ratio ε_c is used to measure the blockage condition of GDL/FF interface, which may lead to water flooding in PEM fuel cell [3]. It is found that the $\varepsilon_{c\text{final}}$ of the middle size but not the biggest droplet is the highest, because the biggest droplet is initially adhered by more ligaments and detaches from the lower surface, as shown in Fig 3c at 0 ms. That exactly indicates the merit of MF flow field on water management, i.e., alleviating water blockage of GDL/FF interface. But the water retention phenomenon maybe a new cause of water flooding.

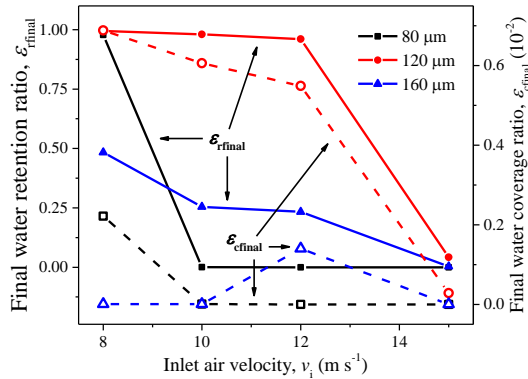


Fig 5 Final water retention and coverage ratio of cases with different droplet sizes and inlet velocities.

3.3 Effects of contact angle on liquid behaviors

The surfaces of conventional channel are normally treated hydrophobic by PTFE, and surface treatment is also important for MF flow field [9-10]. The liquid behaviors with ligaments contact angle of 120° and 150° are exhibited in Fig 6. It is obvious that with the increment of hydrophobicity, the liquid is less likely to adhere to the ligaments. This will accelerate water removal from flow field but will worsen the water coverage condition because the water expelled from GDL may accumulate on GDL/FF interface.

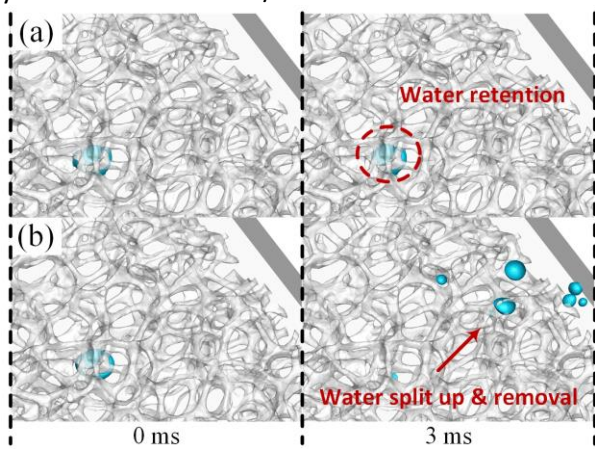


Fig 6 Liquid behaviors in MF flow field with ligaments contact angle of: (a) 120°, (b) 150°.

3.4 Conclusion

In this paper, the real structure of MF flow field is reconstructed based on 3-D CT technology. Then the single- and two-phase flow simulations are carried out. The conclusions are as follows:

- 1) The inhomogeneous distribution of pore structure influences the flow patterns of MF flow field and should be taken into consideration in the simplified geometry reconstruction methods.
- 2) The convective flow and lower permeability of MF flow field contribute to the mass transfer of PEM fuel cell.
- 3) The adhering effect of ligaments alleviates the water coverage condition on GDL surface, while water retention characteristic of MF flow field may become a new cause of water flooding.
- 4) The surface of ligaments should be treated properly considering both water removal from GDL and flow field.

ACKNOWLEDGEMENT

This research is supported by the National Natural Science Foundation of China for Excellent Young Scholars (Grant No. 51622606) and the Natural Science Foundation for Outstanding Young Scholars of Tianjin (grant No. 18JCJQC46700).

REFERENCE

- [1] Wang Y, Chen K S, Mishler J, et al. Appl Energy 2011;88(4): 981-1007.
- [2] Sharaf O Z, Orhan M F. Renewable Sustainable Energy Rev 2014;32: 810-853.
- [3] Park J E, Lim J, Kim S, et al. Electrochim Acta 2018;265: 488-96.
- [4] Yuan W, Tang Y, Yang X, et al. Appl Energy 2012;94: 309-29.
- [5] Carton J G, Olabi A G. Int J Hydrogen Energy 2015;40(16): 5726-38.
- [6] Bao Z, Niu Z, Jiao K. Int J Hydrogen Energy 2019;44(12): 6229-44.
- [7] Cho S C, Wang Y, Chen K S. J Power Sources 2012;206: 119-28.
- [8] Chen J. J Power Sources 2010;195(4): 1122-9.
- [9] Tang Y, Yuan W, Pan M, et al. Int J Hydrogen Energy 2010;35(18): 9661-77.
- [10] Das P K, Grippin A, Kwong A, et al. J Electrochem Soc 2012;159(5): B489-B496.